SPANDIDOS PUBLICATIONS

ONCOLOGY LETTERS 16: 3223-3230, 2018

The impact of exogenous CO releasing molecule CORM-2 on inflammation and signaling of orthotopic lung cancer

LI SHAO[1], CONGYANG LIU[1], SHUHUA WANG[2], JIANNAN LIU[3], LI WANG[1], LIPING LV[1] and YONG ZOU[1]

Departments of [1]Integrated Traditional Chinese and Western Medicine, [2]Information and [3]Medical Oncology, The Affiliated Yantai Yuhuangding Hospital of Qingdao University, Yantai, Shandong 264000, P.R. China

Received November 22, 2017; Accepted June 6, 2018

DOI: 10.3892/ol.2018.9022

Abstract. The present study aimed to evaluate the therapeutic effect of CO-releasing molecule-2 (CORM-2) in an established mouse orthotopic lung cancer model and investigate the underlying mechanism associated with inflammation pathway. A total of 80 mice were randomly divided into two groups with 20 serving as a normal control and 60 used for the orthotopic lung cancer model. The tumor group was either untreated, or administrated with DMSO or CORM-2. The mice were sacrificed at day 7 and 14 post-treatment, and the body weight, and thymus and spleen indices were determined. Pathological analysis was performed with hematoxylin and eosin (HE) staining. Serous inflammatory factors were measured using an ELISA. The expression levels of eukaryotic translation initiation factor 4E, p70S6K and toll-like receptor-4 (TLR4) were quantified by reverse transcription-polymerase chain reaction. The effects of CORM-2 on the phosphoinositide 3-kinase (PI3K)/protein kinase B (Akt)/mammalian target of rapamycin (mTOR), TLR4/nuclear factor (NF)-κB signaling pathways were determined by western blotting. The body weight increased over time in the control group, while it significantly declined in tumor-bearing mice (P<0.05). CORM-2 treatment significantly increased body weight in comparison with the model and DSMO treatment groups (P<0.05). The thymus and spleen indices both reduced in the model and DMSO treatment groups, which was significantly rescued with CORM-2 administration (P<0.05). The HE staining results demonstrated few nodule formations, fibrous hyperplasia and extensive necrosis, which suggested overt inhibitory effects against cancer of CORM-2. The serous contents of tumor necrosis factor-α, interleukin (IL)-1β and IL-6 in the CORM-2 group was significantly lower compared with that in the model and DMSO groups (P<0.05). The ratio of phosphorylated (p-PI3K/PI3K, p-AKT/AKT, p-mTOR/mTOR, p-NF-κB-p65/NF-κB-p65 and expression of TLR4 significantly decreased in the CORM-2 group compared with the model and DMSO groups (P<0.05). To the best of our knowledge, the data in the present study demonstrated *in vivo* for the first time, the therapeutic potential of the CORM complex, which is associated with suppression of inflammation and general protein synthesis.

Correspondence to: Dr Yong Zou, Department of Integrated Traditional and Western Medicine, The Affiliated Yantai Yuhuangding Hospital of Qingdao University, 20 Yuhuangding East Road, Zhifu, Yantai, Shandong 264000, P.R. China
E-mail: doctorsci3@126.com

Key words: non-small cell lung cancer, CO-releasing molecule-2, phosphoinositide 3-kinase/protein kinase B/mammalian target of rapamycin, nuclear factor-κB/toll-like receptor-4

Introduction

Lung cancer is the most common causes of cancer-associated mortality worldwide (1). Approximately 1.8 million people are diagnosed with lung cancer and 1.6 million people succumb to this malignancy every year globally (2). The gross 5-year survival rate of patients with lung cancer varies between 4 and 17% depending on early diagnosis and clinical management (3). Lung cancer is generally divided into two subtypes: Non-small cell lung cancer (NSCLC) and small cell lung cancer (SCLC) based on histological characteristics (4). NSCLC accounts for the majority of clinical cases (5). The etiology of lung cancer is associated with genetic, epigenetic and environmental causes (6). Despite the significant advances in treatments in the last decades, various therapeutic challenges remain (3).

Clinically lung cancer is frequently diagnosed at the late stage and with relative poor prognosis (7). Efforts have been to develop early screening techniques in the past decades. The pioneering project, The National Lung Screening Trial, initiated in 2002 demonstrated promising results, whereby the use of low-dose computed tomography scans resulted in a 20% reduction in lung cancer mortality (8). Currently, surgical removal is the standard procedure for patients with early-stage lung cancer and the 5-year survival rate is relatively promising with an overall survival rate of 50-90% (9). Patients with local advanced NSCLC who are not amenable to surgery are recommended for thoracic radiotherapy combined with chemotherapy (10). Targeted therapy is also currently used in the clinic but is limited to those with well-defined genomic aberrations (11). Unfortunately, patients who receive targeted therapy usually experience rapid recurrence with limited extensions in overall survival. In addition, immunotherapy was used to block tumor immunosuppressive cells and demonstrated clinical benefits, however the rate autoimmune

disorders associated with this treatment is high (7). Therefore, the development of novel therapeutics is still required for the optimal treatment of lung cancer.

Carbon monoxide (CO), primarily from incomplete combustion, is recognized historically as a toxic gas due to its strong affinity to hemoglobin, which inhibits oxygen delivery capacity and causes asphyxial death (12). Increasing evidence has indicated that CO is also physiologically produced as a byproduct of heme degradation by heme oxygenase (HO) endogenously, which serves essential roles in circadian rhythms (13), neural memory (14) and hemodynamic modulation (15). The therapeutic potential of CO was exploited in cardiovascular disease (16), inflammatory disorders (17) and organ transplantation (18). However, to the best of our knowledge, the clinical benefit of CO on human tumors and the likely mode of action have not been extensively investigated. With the introduction of controllable release of CO and insightful elucidation of therapeutic mechanisms in other clinical complications, the anti-tumor effects of CO may be investigated. The present study aimed to establish an orthotopic lung cancer mouse model, investigate the potential application of CO-releasing molecule-2 (CORM-2) *in vivo* and determine the underlying mechanism particularly with respect to the modulation of tumor-associated inflammation.

Materials and methods

Animals. In total, 80 male specific-pathogen-free-grade mice with a mean body weight 18-22 g and 6-8 weeks of age were raised for 1 week in an adaptive phase, purchased from Jinan Pengyue Experimental Animal Breeding Company (Jinan, China). All C57BL/6 mice were maintained at a temperature of 25±5˚C and humidity of 55±5%, wit a light/dark cycle of 12 h, and free access to normal diet and water. All experimental protocols were approved by the Committee of Animal Care and Use of The Affiliated Yantai Yuhuangding Hospital of Qingdao University. All animal studies were performed in strict accordance with the approved protocol.

Orthotopic lung cancer model. Mouse LLC lung cancer cells (CRL-1642; American Type Culture Collection, Manassas, VA, USA) were cultured in high-glucose Dulbecco's modified Eagle's medium supplemented with 10% fetal bovine serum (FBS) (Gibco; Thermo Fisher Scientific, Inc., Waltham, MA, USA) at 37˚C in a 5% CO_2 incubator. The cells were collected when 90% confluence was achieved by centrifugation (3,600 x g, at 4˚C for 10 min) and re-suspended in PBS. Cells with >90% viability were counted with an automatic cell counter (Beckman Coulter, Inc., Brea, CA, USA) then adjusted to the concentration of $4x10^7$/ml, which were mixed with an equal volume of Matrigel (BD Biosciences, Franklin Lakes, NJ, USA) on ice for inoculation at 4˚C as described below.

In total, 80 mice were raised for the present study and 20 served as normal control that received no treatment. The rest were subjected to the orthotopic lung cancer model. The mice were anesthetized with 10 mg/ml chloral hydrate at a dosage of 0.5 ml/10 g (body weight) and positioned with the right lateral side on the operation table. The underarm hair was removed and the skin was prepared with ethanol disinfection. A 5-mm incision was introduced 1.5 cm above the rib arch along the left anterior line, the skin and subcutaneous tissues were separated to expose the chest wall until movement of the lung lobes was visible. The 50 μl mixture of Matrigel and cell suspension were pre-warmed in a micro-syringe at room temperature for 2 min, then was inoculated 3-mm deep in the left lung. The needle was held still in the injection site for a few sec following the injection. The incision was sutured following needle extraction.

Drug treatment. The successfully established tumor-bearing mice were randomly subdivided into the model, DMSO or CORM-2 (Sigma-Aldrich; Merck KGaA, Darmstadt, Germany) treatment groups 7 days post-operation, which were administrated by tail vein injection for 14 consecutive days as follows: Model group with 0.9% saline, 0.2 ml/day; DMSO group with 0.025% DMSO, 0.2 ml/day; CORM-2 group dissolved in 0.025% DMSO, 0.4 mg/kg/day.

Ten mice in each group were sacrificed at day 7 and 14, respectively. The body weights were measured and the blood samples were collected. The thymus and spleen were harvested and weighed to calculate the physiological index. Part of the lung tumor tissues were fixed in 4% neutral formalin for further pathological analysis, and the other part were immediately cryopreserved in liquid nitrogen for future use.

Hematoxylin and eosin (HE) staining. Lung tumor tissues were collected and fixed in 4% neutral formalin at 4˚C for 24 h. Following dehydration in a series of ethanol solutions, samples were paraffin-embedded and sliced into 5-μm thin sections. Slides were deparaffinized in xylene for 10 min three times, and rehydrated by serial soaking in 100% ethanol for 10 min, and 95, 85, 75% ethanol for 5 min each at 25˚C. After 0.1% hematoxylin staining for 10 min at 25˚C and a thorough wash with distilled water for 20 min at 25˚C, the slides were subjected to 0.5% eosin staining for another 3 min at 25˚C. Subsequently, the slides were incubated in 95% anhydrous ethanol for 5 min twice and in xylene solution for 10 min at 25˚C. Then, the slides were mounted in neutral resin for optical microscopy (Olympus, Japan) examination at x100 magnification.

ELISA. The supernatants were collected from the rat lung tissue homogenate, and the concentration of inflammatory factors tumor necrosis factor (TNF)-α (PT512; Beyotime Institute of Biotechnology, Haimen, China), interleukin (IL)-1β (PI301; Beyotime Institute of Biotechnology) and IL-6 (PI326; Beyotime Institute of Biotechnology) were measured using an ELISA kit according to the manufacturer's protocol.

RT-PCR. Total RNA was extracted from indicated samples with TRIzol reagent (Life Technologies; Thermo Fisher Scientific, Inc.) The total RNA extraction purity, determined using UV spectrophotometry (Bio-Rad Laboratories, Inc., Hercules, CA, USA) at OD260/OD280, was between 1.8 and 2.0. The first strand cDNA was synthesized using the PrimeScript RT reagent kit (Takara Biotechnology Co., Ltd., Dalian, China) according to the manufacturer's protocol. RT-PCR was conducted with the SYBR Green Master kit (Promega Corporation, Madison, WI, USA) in according to the manufacturer's protocol. The primers used in the present study listed

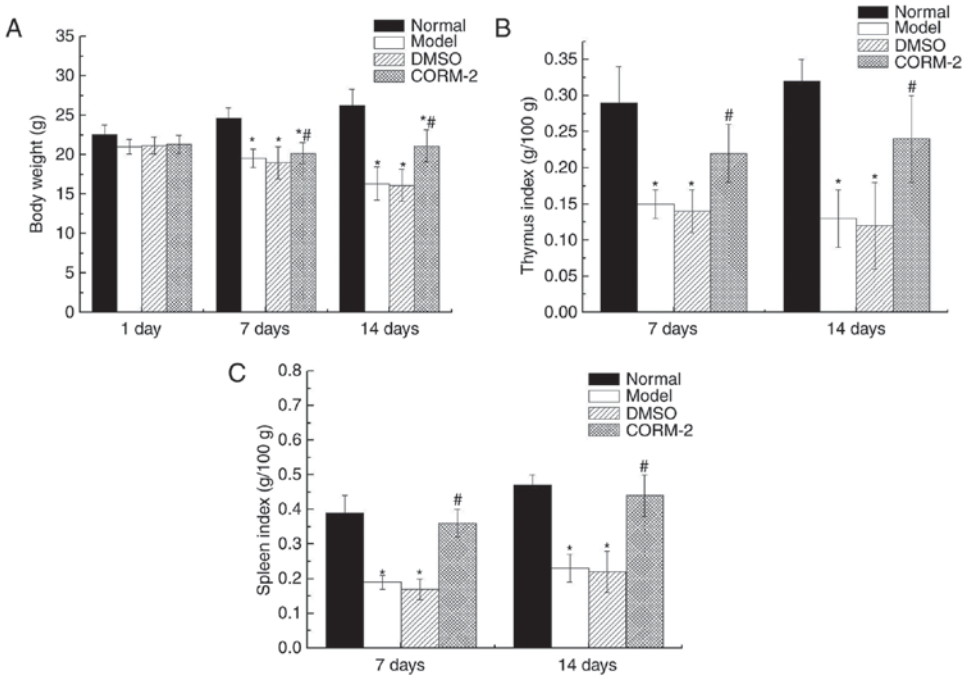

Figure 1. Changes in body weight, thymus and spleen index in mouse models. Mice were sacrificed, and (A) body weights were determined at day 1, 7 and 14 after the indicated treatment in the control and orthotopic lung tumor model. (B) Thymus and (C) spleen were also weighed at day 7 and 14. Each bar represents the mean ± standard deviation of 10 mice. *P<0.05 (model or DMSO vs. control), #P<0.05 (CORM-2 vs. model). CORM-2, CO-releasing molecule-2.

as follows: Eukaryotic translation initiation factor 4E (4E-BP1; Gene ID: 1978) forward, 5'-GGACCAGCCGTAGGAC-3' and reverse, 5'-TGAGTGAGGAGCAGGAC-3'; p70S6K (Gene ID: 114294) forward, 5'-TACTTCGGGTACTTGGTAA-3' and reverse, 5'-GATGAAGGGATGCTTTACT-3'; Toll-like receptor (TLR)4 (Gene ID: 21898) forward, 5'-TTCTTCTCC TGCCTGACACC-3' and reverse, 5'-CTTTGCTGAGTTTCT GATCCAT-3'; GAPDH (Gene ID: 2597) forward, 5'-CCA TCACCATCTTCCAGGAG-3' and reverse, 5'-CCTGCTTCA CCACCTTCTTG-3'. The bands were analyzed using ImageJ software (version 2.0; National Institutes of Health, Bethesda, MD, USA). The relative expression was calculated and normalized to GAPDH. The results are representative of at least three independent experiments.

Western blot analysis. The total protein was extracted with radioimmunoprecipitation assay lysis buffer (Beyotime Institute of Biotechnology) from lung tissues and quantified using a Coomassie brilliant blue assay (Pierce; Thermo Fisher Scientific, Inc.). Approximately 20 μg of total protein was electrophoresed on using 10% SDS-PAGE and transferred to polyvinylidene difluoride membranes at 4˚C. The membranes were blocked with 5% bovine serum albumin (Gibco; Thermo Fisher Scientific, Inc.) solution for 1.5 h at 4˚C and hybridized with primary antibodies against phosphorylated (p)-phosphoinositide 3-kinase (PI3K; cat. no. 4228; 1:1,000), PI3K (cat. no. 4255; 1:1,000), p-protein kinase B (Akt; cat. no. 9272; 1:1,000), Akt (cat. no. 9611; 1:1,000) (Cell Signaling Technology, Inc., Danvers, MA, USA), p-mammalian target of rapamycin (mTOR; cat. no. ab84400; 1:1,000), mTOR (ab109268; 1:1,000), p-NF-κB-p65 (ab86299; 1:2,000), NF-κB-p65 (ab16502; 1:1,000), TLR4 (ab13556; 1:500) (Abcam, Cambridge, UK) at 4˚C overnight. The phosphorylation sites of PI3K, Akt, mTOR and NF-κB-p65 are Lys802, Ser308, Ser2448 and Ser536, respectively. The membranes were rigorously washed with TBST (Tris-buffered saline plus 0.1% Tween-20) at room temperature for 30 min and then incubated with horseradish peroxidase-conjugated goat anti-rabbit antibodies (ab6721; 1:5,000; Abcam) for 2 h at room temperature. The membranes were washed again with TBST and visualized using an enhanced chemiluminiscence kit (Bio-Rad Laboratories, Inc., Hercules, CA, USA) according to the manufacturer's protocol. Each protein band was quantified via densitometry using Quantity One software (version 4.62; Bio-Rad Laboratories, Inc., Hercules, CA, USA) and normalized to the loading control (GAPDH).

Statistical analysis. Data from three independent experiments were subjected to statistical analysis using SPSS 19.0 software (IBM Corp., Armonk, NY, USA), and all results are presented as mean ± standard deviation. Multiple group comparison analysis was performed using a one-way ANOVA followed by Fisher's least significant difference post-hoc test. Student's t-test was used for pairwise group comparisons. The statistical significances between data sets are expressed as P-values, and P<0.05 was considered to indicate a statistically significant difference.

Results

CORM-2 treatment increases the body weight and thymus/spleen index of lung tumor-bearing mice. First, the impact of CORM-2 treatment on mice body weight and thymus/spleen index was examined at days 0, 7 and 14, and was considered as an approximate health measurement (Fig. 1). The results demonstrated an increase in body weight over time in control mice, while a significant loss in body weight with

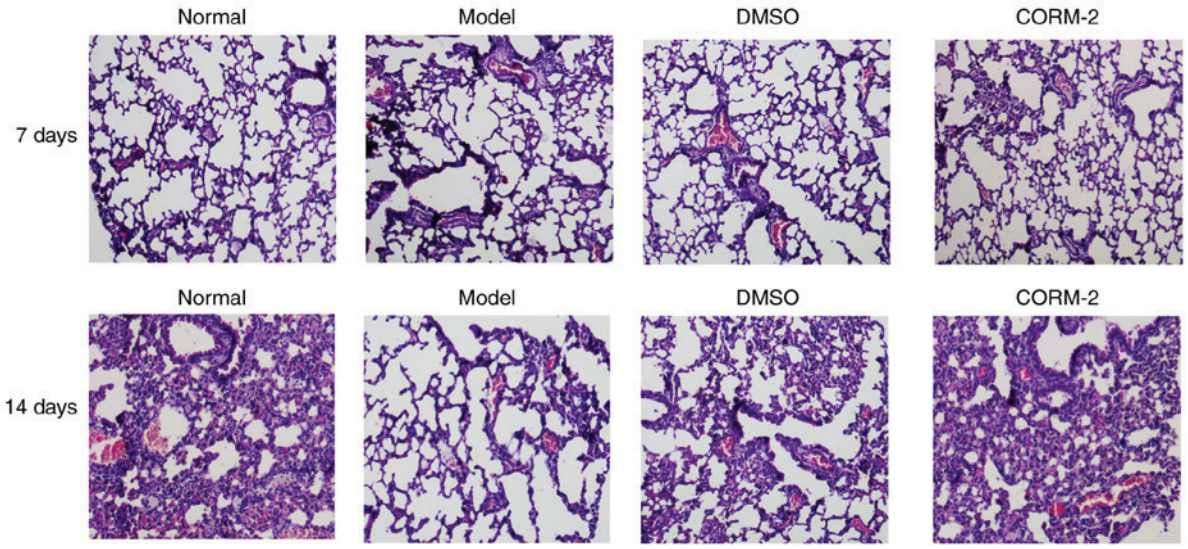

Figure 2. CORM-2 inhibits the pathological features of orthotopic lung tumors. Hematoxylin and eosin staining of lung tissue sections from mice, which were subjected to optical microscopy (magnification, x100). CORM-2, CO-releasing molecule-2.

tumor progression was observed in the orthotopic lung tumor groups (P<0.05). In comparison with model group, DMSO treatment elicited no significant difference in respect to body weight, while remarkable elevation in response to CORM-2 administration (P<0.05).

Development of the thymus and spleen was also evaluated simultaneously. The organ weight was much lower in model and DMSO mice, which significantly increased upon CORM-2 management (P<0.05) and to a certain extent was comparable with control mice. No significant differences were observed between the model and DMSO treatment groups. These results demonstrated the inhibitory effect of CORM-2 on tumor progression.

Histopathological characteristics in response to CORM-2 treatment. Next, the pathological sections were examined using HE staining of the lung tissue harvested from the mice (Fig. 2). Clear bronchial pulmonary alveolus structures, intact epithelia, and few inflammatory cell infiltrations to the bronchial walls and blood vessels were observed in all normal mice (n=20). There were invisible huge emboli in the alveoli of model and DMSO mice under an optical microscope (n=20). The cancer cell nucleus was extensively stained dark blue and heterogeneously deformed. In contrast, there were no evident cancer emboli in CORM-2 treated mice (n=19), which was accompanied with extensive fibrous hyperplasia, bleeding and necrosis. The pathologic analysis suggested an intense inhibitory action of CORM-2 on orthotopic lung tumor in site.

CORM-2 suppresses the expression of TNF α, IL-1β and IL-6. Cancer progression s frequently accompanied with a severe inflammatory response (19). Therefore, the present study aimed to determine the effect of CORM-2 treatment on inflammation-associated factors (Fig. 3). ELISA was performed to detect serous contents of TNF α, IL-1β and IL-6. Strong inflammatory responses were invoked in model and DSMO treatment groups at day 7, which persisted at a high level at day 14 (P<0.05). CORM-2 treatment caused a significant reduction in these factors at day 7, and this effect was further increased by day 14 (P<0.05). The serous concentrations of TNF α, IL-1β and IL-6 were nearly back to normal at day 14, which indicated inflammation reversal via CORM-2 in these models.

CORM-2 inhibits the expression of 4E-BP1, p70S6K and TLR4. Deregulation of p70S6K pathway has been reported to be associated with cancer progression (20). TLR4 is a member of the TLR family, which is essential in pathogen recognition and activation of innate immunity. Overexpression of TLR4 is involved in the activation of cancer cells via the production of cell survival, pro-angiogenesis and pro-inflammatory signals, which subsequently stimulate tumor cell proliferation and suppress antitumor immunity by recruiting immunomodulatory cells to the microenvironment (21). The influential effect of CORM-2 on 4E-BP1, p70S6K and TLR4 were examined (Fig. 4).

The RT-PCR results revealed a higher level of 4E-BP1, p70S6K and TLR4 in orthotopic lung tumor models compared with the control (P<0.05) at day 7, which indicated active proliferation associated with tumor growth. However, CORM-2 treatment led to a significant decrease (P<0.05). The expression of 4E-BP1, p70S6K and TLR4 increased persistently until day 14 in the model group, which was significantly reversed by CORM-2 treatment (P<0.05). DMSO solvent treatment exhibited no significant impact on the expression of the aforementioned genes compared with the model group.

CORM-2 treatment inhibits the PI3K/Akt/mTOR and NF-κB/TLR signaling pathway. The PI3K/Akt/mTOR and NF-κB/TLR pathways are among the most frequently dysregulated pathways involved in tumorigenesis and tumor progression, and are important players in cell proliferation and inflammation (22,23). The present study aimed to determine the modulation of these pathways during tumor progression and treatment with CORM-2.

The tissue content of p-PI3K, PI3K, p-AKT, AKT, p-mTOR and mTOR were measured by western blotting, and the

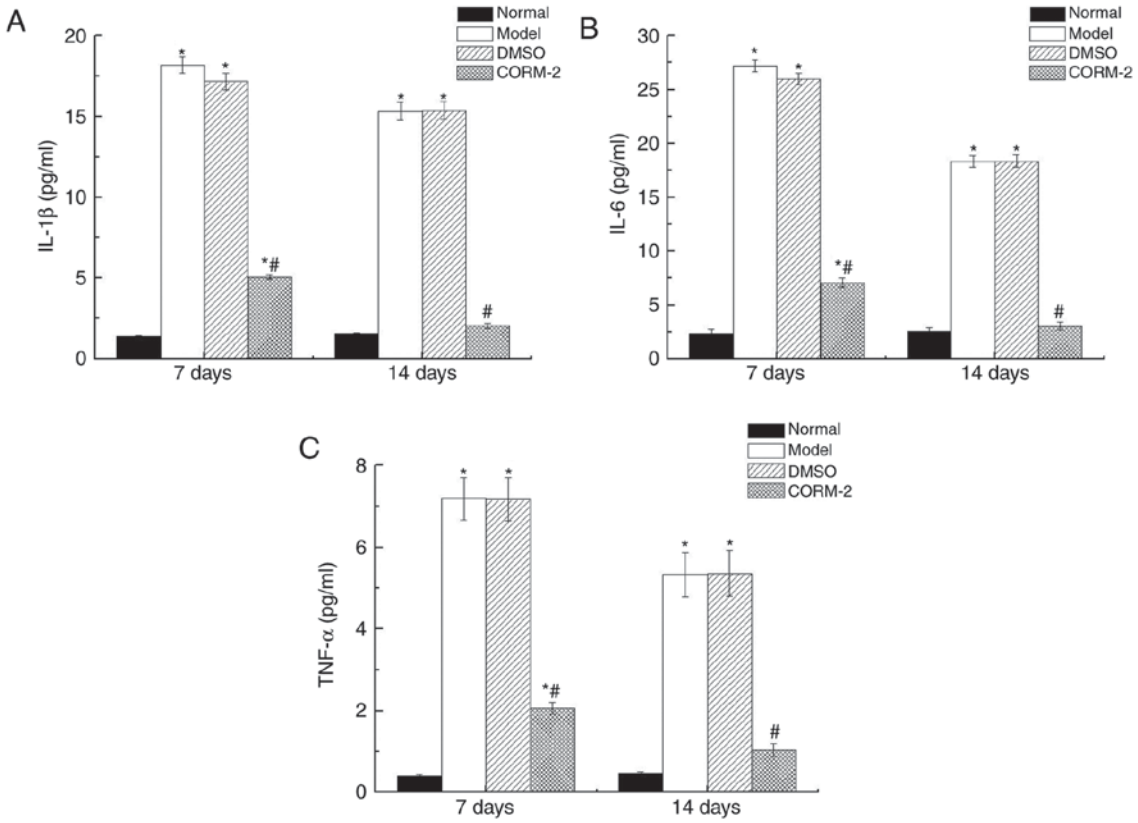

Figure 3. CORM-2 suppresses serous inflammatory factors. Serous contents of (A) IL-1β, (B) IL-6 and (C) TNFα were determined using an ELISA. Each bar represents the mean of 10 mice in the indicated groups. *P<0.05 (model or DMSO vs. control), #P<0.05 (CORM-2 vs. model). IL, interleukin; TNFα, tumor necrosis factor α; CORM-2, CO-releasing molecule-2.

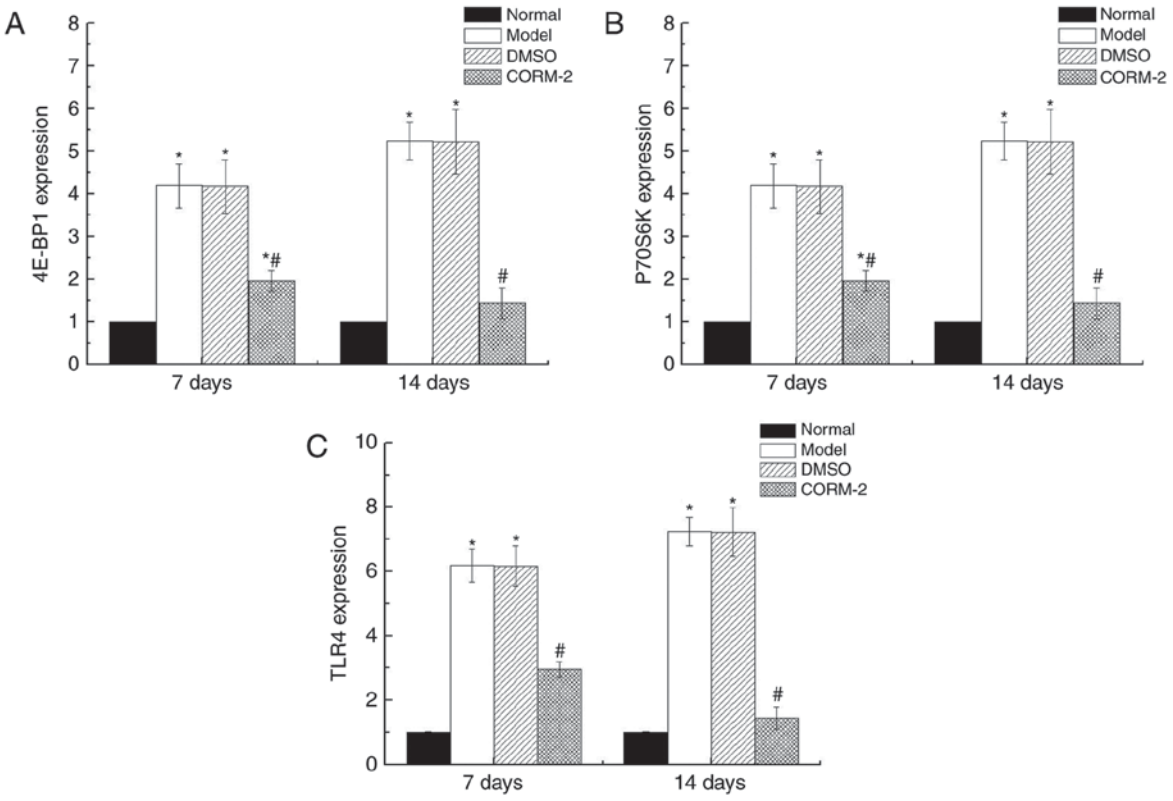

Figure 4. CORM-2 decreases the expression of 4E-BP1, p70S6K and TLR4. The relative expression of (A) 4E-BP1, (B) p70S6K and (C) TLR4 in indicated mice were quantified by reverse transcription-quantitative polymerase chain reaction and normalized to GAPDH. Each bar represents the mean fold change of 10 mice. *P<0.05 (model or DMSO vs. control), #P<0.05 (CORM-2 vs. model). TLR-4, toll-like receptor-4; CORM-2, CO-releasing molecule-2; 4E-BP1, eukaryotic translation initiation factor 4E.

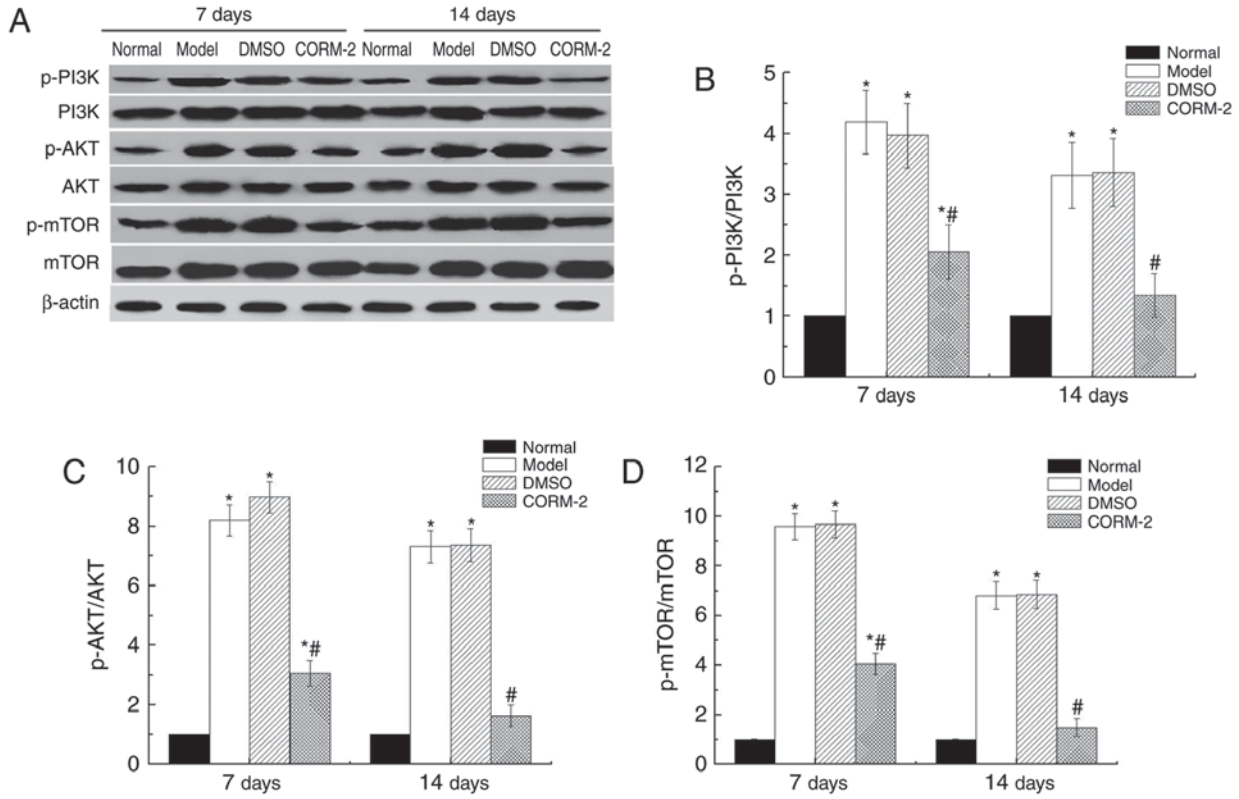

Figure 5. CORM-2 inhibits phosphorylation of PI3K, AKT and mTOR. (A) The relative content of p-PI3K, PI3K, p-AKT, AKT, p-mTOR and mTOR in the indicated mice were determined by immunoblotting. The band intensity was analyzed with densitometry and normalized to β-actin. (B) p-PI3K and PI3K; (C) p-AKT and AKT; (D) p-mTOR and mTOR. Each bar represents the mean ± standard deviation of 10 mice. *P<0.05 (model or DMSO vs. control), #P<0.05 (CORM-2 vs. model). PI3K, phosphoinositide 3-kinase; Akt, protein kinase B; mTOR, mammalian target of rapamycin; CORM-2, CO-releasing molecule-2; p, phosphorylated.

results are presented as the ratio between phosphorylated and non-phosphorylated forms of PI3K, AKT and mTOR (Fig. 5). Phosphorylation was significantly elevated in tumor-bearing mice, which was consistent with active proliferation and tumor progression. Following treatment with CORM-2, the phosphorylation levels were significantly reduced and the AKT pathway was downregulated. Administration of CORM-2 for 14 consecutive days almost completely abolished the phosphorylation of these factors and activation of the PI3K/AKT/mTOR signaling pathway. These results indicated that CORM-2 exhibited potential as a tumor suppressor.

Next, the expression levels of NF-κB/TLR4 signaling pathway-associated proteins were examined. Phosphorylation of p65 enhanced its nuclear retention and transcription activity. Elevated phosphorylation of p65 in orthotopic allografts was evident, which declined upon treatment with CORM-2. Administration for 14 days was sufficient to restore the basic physiological phosphorylation level. The same trend was observed for TLR4 following CORM-2 treatment (Fig. 6). These results suggested that CORM-2 suppressed tumor progression via the NF-κB/TLR4 signaling pathway.

Discussion

Although CO is considered a poison, there is increasing awareness regarding the physiological function *in vivo* and therapeutic potential of CO (24). Endogenous CO is produced during the degradation of heme, which is catalyzed by the HO enzymes for biliverdin generation and iron release (25). Highly diffusive CO gas exhibits strong affinity to transition metals, with facilitates its binding to hemoprotein in the circulation and eventual exhalation via the lungs. The clinical benefits of low dose CO have been evaluated in several different disease models. The first phase I trial of the Covox DS delivery device revealed a safe and controllable way for CO administration with assessment of carboxy-hemoblobin in the blood (26). Thereafter, CORMs were developed to mimic the biological action of endogenous CO in a controlled-release manner *in vivo* (27). Among which, CORM-2 was the first synthesized lipid-soluble metal carbonyl complex, tricarbony idichlororuthenium (II) dimer $[Ru(CO)_3Cl_2]_2$, and releasing CO *in vivo* and exerting typical CO-mediated pharmacological effects, including vasodilation and hypotension (28). Accumulating evidence have suggested anti-inflammatory and anti-oxidative activity of CORM-2, but its potential anti-tumor activity has not been fully determined.

In the present study, an orthotopic allograft of mice lung cancer was established. CORM-2 was administrated by tail vein injection at s dosage of 0.4 mg/kg/day for 14 consecutive days. This dosage was well tolerated and no toxicity was observed until the mice were sacrificed due to tumor overgrowth. Allograft tumor progression caused critical body weight loss, and enlargement of the thoracic and spleen, this adverse effect was significantly reversed by CORM-2 administration. Pathological examination demonstrated evident mitigation of emboli formation, accompanied with extensive

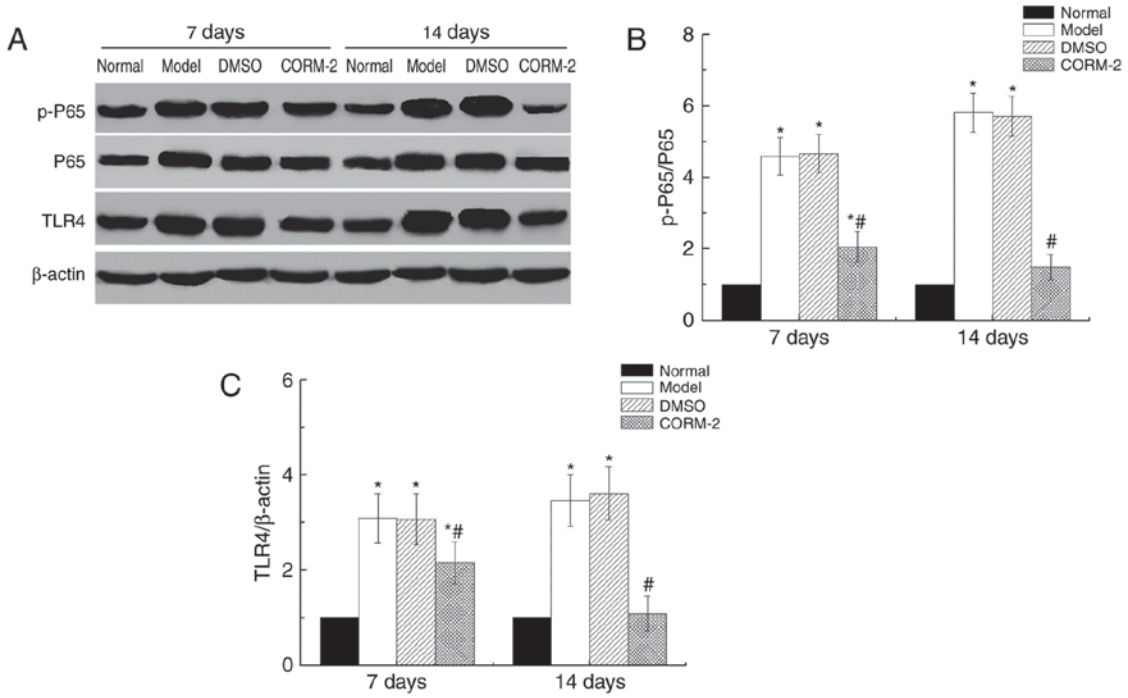

Figure 6. CORM-2 inhibits NF-κB/TLR4 pathway. (A) The relative content of p-P65, P65, TLR4 in indicated mice were determined by immunoblotting. The bands intensity was analyzed with densitometry and normalized to β-actin. (B) p-P65 and P65; (C) TLR4. Each bar represents the mean ± standard deviation of 10 mice. *P<0.05 (model or DMSO vs. control), #P<0.05 (CORM-2 vs. model). CORM-2, CO-releasing molecule-2; p, phosphorylated; TLR-4, toll-like receptor-4; NF-κB, nuclear factor-κB.

fibrous hyperplasia, local hemorrhage and necrosis. These phenotypes suggested efficient tumor suppression activity associated with CORM-2 treatment.

The AKT/mTOR signaling pathway is frequently aberrantly activated in human lung cancer (29), and transmits upstream proliferation signals via a phosphorylation cascade, eventually stimulating the transcription of effectors downstream. The allograft mice in the present study demonstrated consistent changes of intensive phosphorylation signaling of PI3K, AKT and mTOR in the lung tumor model, which indicated highly active biological synthesis and malignant proliferation. Administration of CORM-2 significantly and efficiently blocked this central proliferation pathway in a tumor-specific manner.

A previous study indicated that inflammation serves important roles in tumor biology, including in the initiation, progression, metastasis, recurrence and resistance of tumors (30). Through autocrine and paracrine signaling pathways, the local and recruited inflammatory cells irrigate the pro-proliferative tumor microenvironment. However, the signal molecules secreted by inflammatory cells mediate the second wave of recruitment of tumor suppressive immune cells, including macrophages and T cells, which in turn are exploited by cancer cells for immunosuppression (31). Therefore, the peripheral inflammatory factors in the blood, lymph and urine are usually rich sources of indicators for detection of tumor progression. In the present study, the circulatory concentrations of TNF-α, IL-6 and IL-1β were monitored, where were significantly elevated with the progression of the lung tumor, and efficiently inhibited by CORM-2 treatment. These results supported a potential anti-tumor mechanism of CORM-2 via suppression of the inflammatory reaction in tumors.

Tumor progression per se is an energy-consuming process, which heavily relies on vast biological materials *de novo* synthesis. It has been well established that 4E-BP1 encodes a critical translation repressor protein, which interacts with eukaryotic translation initiation factor 4E and impedes recruitment of 40S ribosomal subunits to the 5'end of mRNAs and successful assembly of functional 80S ribosome (32). p70S6K encodes a member of the ribosomal S6 kinase family of serine/threonine kinases, which responds to mTOR signaling and activation by phosphorylation to promote protein synthesis, cell growth, and cell proliferation (33). In this study, we monitored the expression change of 4E-BP1 and p70S6K to measure the intracellular activity of total translation. The present data suggested the extremely high translational rate in orthotopic allograft, which was significantly suppressed by CORM-2 administration. In addition to the inhibitory effect on tumor associated inflammation, our data also indicated an alternative and simultaneous anti-tumor activity of CORM-2 via limiting protein synthesis.

In conclusion, in the present study we exploited the potential clinical value of CORM-2 and demonstrated the anti-tumor activity of CORM-2 in the orthotopic allograft lung tumor mice model. Administration of CO from CORM-2 complex in a controllable manner at physiological comparable concentration suppressed local inflammation reaction and the central intracellular protein synthesis signaling, which eventually inhibited aberrant cell proliferation and malignant growth. To the best of our knowledge, the data in the current study demonstrated *in vivo*, the therapeutic potential of CORM in the treatment of lung tumor for the first time, and warrants further investigation *in vitro*, *in vivo* and clinically.

Acknowledgements

Not applicable.

Funding

No funding was received.

Availability of data and materials

All data collected or analyzed during this study are included in this article.

Authors' contributions

LS, YZ participated in the sequence alignment. CL, SW, JL, LW and LL carried out the immunoassays. LS and CL participated in the design of the study and performed the statistical analysis. LS SW, JL, LW and LL conceived of the study and participated in its design and coordination. LS drafted the manuscript. YZ helped to check the manuscript. All authors read and approved the final manuscript.

Ethics approval and consent to participate

This study was approved by Ethics Committee of the Affiliated Yantai Yuhuangding Hospital of Qingdao University.

Patient consent for publication

Not applicable.

Competing interests

The authors declare that they have no competing interests.

References

1. Lei L, Huang Y and Gong W: miR-205 promotes the growth, metastasis and chemoresistance of NSCLC cells by targeting PTEN. Oncol Rep 30: 2897-2902, 2013.
2. Siegel RL, Miller KD and Jemal A: Cancer statistics, 2016. CA Cancer J Clin 66: 7-30, 2016.
3. Hirsch FR, Scagliotti GV, Mulshine JL, Kwon R, CurranWJ Jr, Wu YL and Paz-Ares L: Lung cancer: Current therapies and new targeted treatments. Lancet 389: 299-311, 2017.
4. Rabe KF: Lung cancer staging: A true story. Lancet Respir Med 3: 258-259, 2015.
5. Zalcman G, Bergot E, Creveuil C, Levallet G and Lechapt E: Integrating biomarkers into clinical trials: Methodological issues for a new paradigm in nonsmall cell lung cancer. Curr Opin Oncol 23: 106-111, 2011.
6. Baranov VS, Glotov OS and Baranova EV: Genetic and epigenetic news in gerontology. Adv Gerontol 27: 247-256, 2014.
7. Tartour E and Zitvogel L: Lung cancer: Potential targets for immunotherapy. Lancet Respir Med 1: 551-563, 2013.
8. National Lung Screening Trial Research Team, Aberle DR, Adams AM, Berg CD, Black WC, Clapp JD, Fagerstrom RM, Gareen IF, Gatsonis C, Marcus PM and Sicks JD: Reduced lung-cancer mortality with low-dose computed tomographic screening. N Engl J Med 365: 395-409, 2011.
9. Goldstraw P, Chansky K, Crowley J, Rami-Porta R, Asamura H, Eberhardt WE, Nicholson AG, Groome P, Mitchell A, Bolejack V, *et al*: The IASLC lung cancer staging project: Proposals for revision of the TNM stage groupings in the forthcoming (Eighth) Edition of the TNM classification for lung cancer. J Thorac Oncol 11: 39-51, 2016.
10. Curran WJ Jr, Paulus R, Langer CJ, Komaki R, Lee JS, Hauser S, Movsas B, Wasserman T, Rosenthal SA, Gore E, *et al*: Sequential vs. concurrent chemoradiation for stage III non-small cell lung cancer: Randomized phase III trial RTOG 9410. J Natl Cancer Inst 103: 1452-1460, 2011.
11. Tsao AS, Scagliotti GV, Bunn PA Jr, Carbone DP, Warren GW, Bai C, de Koning HJ, Yousaf-Khan AU, McWilliams A, Tsao MS, *et al*: Scientific advances in lung cancer 2015. J Thorac Oncol 11: 613-638, 2016.
12. Douglas CG, Haldane JS and Haldane JB: The laws of combination of haemoglobin with carbon monoxide and oxygen. J Physiol 44: 275-304, 1912.
13. Boehning D and Snyder SH: Circadian rhythms. Carbon monoxide and clocks. Science 298: 2339-2340, 2002.
14. Zhuo M, Small SA, Kandel ER and Hawkins RD: Nitric oxide and carbon monoxide produce activity-dependent long-term synaptic enhancement in hippocampus. Science 260: 1946-1950, 1993.
15. Kobayashi A, Ishikawa K, Matsumoto H, Kimura S, Kamiyama Y and Maruyama Y: Synergetic antioxidant and vasodilatory action of carbon monoxide in angiotensin II-induced cardiac hypertrophy. Hypertension 50: 1040-1048, 2007.
16. Durante W, Johnson FK and Johnson RA: Role of carbon monoxide in cardiovascular function. J Cell Mol Med 10: 672-686, 2006.
17. Nakahira K and Choi AM: Carbon monoxide in the treatment of sepsis. Am J Physiol Lung Cell Mol Physiol 309: L1387-L1393, 2015.
18. Akamatsu Y, Haga M, Tyagi S, Yamashita K, Graça-Souza AV, Ollinger R, Czismadia E, May GA, Ifedigbo E, Otterbein LE, *et al*: Heme oxygenase-1-derived carbon monoxide protects hearts from transplant associated ischemia reperfusion injury. FASEB J 18: 771-772, 2004.
19. Nakamura K and Smyth MJ: Targeting cancer-related inflammation in the era of immunotherapy. Immunol Cell Biol 95: 325-332, 2017.
20. Azaro A, Rodon J, Calles A, Braña I, Hidalgo M, Lopez-Casas PP, Munoz M, Westwood P, Miller J, Moser BA, *et al*: A first-in-human phase I trial of LY2780301, a dual p70 S6 kinase and Akt Inhibitor, in patients with advanced or metastatic cancer. Invest New Drugs 33: 710-719, 2015.
21. Chung YH and Kim D: Enhanced TLR4 expression on colon cancer cells after chemotherapy promotes cell survival and epithelial-mesenchymal transition through phosphorylation of GSK3β. Anticancer Res 36: 3383-3394, 2016.
22. Mundi PS, Sachdev J, McCourt C and Kalinsky K: AKT in cancer: New molecular insights and advances in drug development. Br J Clin Pharmacol 82: 943-956, 2016.
23. Rinkenbaugh AL and Baldwin AS: The NF-kB pathway and cancer stem cells. Cells 5: E16, 2016.
24. Motterlini R and Otterbein LE: The therapeutic potential of carbon monoxide. Nat Rev Drug Discov 9: 728-743, 2010.
25. Tenhunen R, Marver HS and Schmid R: The enzymatic conversion of heme to bilirubin by microsomal heme oxygenase. Proc Natl Acad Sci USA 61: 748-755, 1968.
26. Dercho RA, Nakatsu K, Wong RJ, Stevenson DK and Vreman HJ: Determination of in vivo carbon monoxide production in laboratory animals via exhaled air. J Pharmacol Toxicol Methods 54: 288-295, 2006.
27. Foresti R, Bani-Hani MG and Motterlini R: Use of carbon monoxide as a therapeutic agent: promises and challenges. Intensive Care Med 34: 649-658, 2008.
28. Motterlini R, Clark JE, Foresti R, Sarathchandra P, Mann BE and Green CJ: Carbon monoxide-releasing molecules: Characterization of biochemical and vascular activities. Circ Res 90: E17-E24, 2002.
29. Xie J, Wang X and Proud CG: mTOR inhibitors in cancer therapy. F1000Res 5: F1000 Faculty Rev-2078E, 2016.
30. Crusz SM and Balkwill FR: Inflammation and cancer: Advances and new agents. Nat Rev Clin Oncol 12: 584-596, 2015.
31. Cho WC, Kwan CK, Yau S, So PP, Poon PC and Au JS: The role of inflammation in the pathogenesis of lung cancer. Expert Opin Ther Targets 15: 1127-1137, 2011.
32. Wang R, Ganesan S and Zheng XF: Yin and yang of 4E-BP1 in cancer. Cell Cycle 15: 1401-1412, 2016.
33. Riedl A, Schlederer M, Pudelko K, Stadler M, Walter S, Unterleuthner D, Unger C, Kramer N, Hengstschläger M, Kenner L, *et al*: Comparison of cancer cells in 2D vs. 3D culture reveals differences in AKT-mTOR-S6K signaling and drug responses. J Cell Sci 130: 203-218, 2017.